

FINITE ELEMENT MODELLING OF THE CHECKING OF WOOD EXPOSED TO ACCELERATED WEATHERING

S.G. Ribarits and P.D. Evans

Centre for Advanced Wood Processing, University of British Columbia, Vancouver, BC, Canada, V6T 1Z4

Summary

The surface checking that develops when wood is exposed to the weather reduces the visual appeal of treated wood products and can reduce the effectiveness of preservative treatments. There is strong interest in developing solutions to this problem and also a growing realization that such solutions may evolve from a deeper understanding of the mechanisms responsible for surface checking. In this paper we describe a two-dimensional finite element model that couples moisture diffusion, dimensional change and the development of strains in wooden decking boards exposed to accelerated weathering. The model successfully predicts the strains that cause checks to form in decking boards exposed to accelerated weathering. High tension strains develop at the surface of boards, as expected, but we also observe high strains in the rays and in the core of boards. Such strains explain how checks propagate radially and why internal checks can develop in decking boards. These internal checks may create large cracks when they coalesce with surface checks. In summary, the model we have developed has provided useful insights into the mechanisms responsible for the checking of wood. Further development of the model could provide additional insights and allow it to be used as a tool to optimize the weathering cycles of devices designed to accelerate the checking of wood, or to virtually screen chemical or physical treatments designed to reduce the checking of wooden decking boards.

1. Introduction

The market for timber decking in the USA is valued at US\$ 2.8 billion per annum. Timber decks extend household living areas and consumers expect the decks to be visually appealing as well as structurally sound. Defects that develop in decks following installation such as surface weathering checks and larger cracks reduce the visual appeal of decks, and, accordingly, there is evidence that treated timber decks are replaced because of the occurrence of such defects (McQueen and Stevens 1998). This dissatisfaction with timber decks is being exploited by manufacturers of plastic and plastic-wood decking who claim that their products do not check or split. These plastic decking boards have captured at least 15% of the total market for decking boards in North America at the expense of wooden decking boards (Markarian 2005).

The reason for the checking of decking boards exposed outdoors is understood in qualitative terms. The upper surfaces of decking boards exposed outdoors are subjected to frequent wetting and drying. Wood beneath the exposed surface dries more slowly than at the surface and hence surface shrinkage will be restrained by sub-surface layers whose moisture content exceeds the fiber saturation point, and by fasteners which reduce the tendency of boards to warp. Such restraint of shrinkage will result in the development of surface tension stresses. The size of these stresses depends on the magnitude of the shrinkage strains that develop in the surface layers, but if these stresses exceed the tensile strength of the wood perpendicular to the grain then checks will develop. This qualitative description of checking is similar to those used to explain the checking of wood during kiln drying (Schniewind 1963). The checking of wood during kiln drying has also been described quantitatively using mathematical models (Oliver 1986, Salin 1992). These models provide a means of thinking more systematically about the problem of checking of wood during drying. Some of the models can also simulate the effects of drying parameters and wood characteristics on checking without the need for costly physical experiments. Similar models have not been developed for the checking of wood exposed to artificial or natural weathering.

In this paper we describe a two-dimensional finite element model that couples moisture diffusion, dimensional change and the development of strains in wooden decking boards exposed to accelerated weathering. We describe the insights that the model provides into the mechanisms responsible for the checking of wood and suggest how the model can be improved.

2. Methodology

It is well established that changes in moisture content can produce deformations (strains) that cause checks to form in wood (Mackay 1973, Oliver 1986). This aspect of wood checking can be considered structural and is governed by the laws of continuum mechanics and the constitutive relationships for wood. In turn, changes in moisture content are the result of water diffusing into and out of the interior regions of wood. As diffusion is governed by the laws of mass transfer it is clear that checking in wood is the result of two coupled physical processes. A finite element formulation that encompasses both of these processes is presented in the following sections.

2.1. Structural Model

In wood subject to changing moisture content, the total mechanical strain that leads to checking is the sum of the strains due to elastic and visco-elastic deformations, moisture content changes and the mechano-sorptive effect (Salin 1992). While it is desirable (and the goal of future work) to incorporate all these strain components into the deck checking model, it was decided that

initial insights could be gained at reduced computational cost by neglecting visco-elastic deformations and the mechano-sorptive effect. Hence the total mechanical strain rate was taken to be

$$\dot{\boldsymbol{\varepsilon}} = \dot{\boldsymbol{\varepsilon}}_e + \dot{\boldsymbol{\varepsilon}}_w \quad (1)$$

where $\boldsymbol{\varepsilon}$ is the total mechanical strain; $\boldsymbol{\varepsilon}_e$, the elastic strain; and $\boldsymbol{\varepsilon}_w$, the moisture induced strain.¹

The elastic strain component in (1) is

$$\dot{\boldsymbol{\varepsilon}}_e = \mathbf{C}\dot{\boldsymbol{\sigma}} + \dot{\mathbf{C}}\boldsymbol{\sigma} \quad (2)$$

where $\boldsymbol{\varepsilon}_e$ is the elastic strain vector; $\boldsymbol{\sigma}$, the stress vector; and \mathbf{C} , the elastic compliance matrix. For a general three-dimensional state of stress, these are written

$$\boldsymbol{\varepsilon}_e = \begin{bmatrix} \varepsilon_t & \varepsilon_r & \varepsilon_l & \gamma_{tr} & \gamma_{tl} & \gamma_{rl} \end{bmatrix}^T \quad (3)$$

$$\boldsymbol{\sigma} = \begin{bmatrix} \sigma_t & \sigma_r & \sigma_l & \tau_{tr} & \tau_{tl} & \tau_{rl} \end{bmatrix}^T \quad (4)$$

$$\mathbf{C} = \begin{bmatrix} 1/E_t & -\nu_{rt}/E_r & -\nu_{lt}/E_l & 0 & 0 & 0 \\ -\nu_{tr}/E_t & 1/E_r & -\nu_{lr}/E_l & 0 & 0 & 0 \\ -\nu_{tl}/E_t & -\nu_{rl}/E_r & 1/E_l & 0 & 0 & 0 \\ 0 & 0 & 0 & 1/G_{tr} & 0 & 0 \\ 0 & 0 & 0 & 0 & 1/G_{tl} & 0 \\ 0 & 0 & 0 & 0 & 0 & 1/G_{rl} \end{bmatrix} \quad (5)$$

In the elastic compliance matrix (5) the terms E_t , E_r and E_l are the elastic moduli in the three orthotropic directions (t , transverse; r , radial; and l , longitudinal) and G_{tr} , G_{tl} and G_{rl} are the shear moduli in the three (tr , tl and rl) orthotropic planes. The terms ν_{rt} , ν_{tr} , ν_{lt} , ν_{tl} , ν_{lr} , and ν_{rl} are the Poisson's ratios. From symmetry of the compliance matrix, it follows that $\nu_{rt} = (E_r/E_t)\nu_{tr}$, $\nu_{lt} = (E_l/E_t)\nu_{tl}$ and $\nu_{lr} = (E_l/E_r)\nu_{rl}$.

It has been observed that the elastic and shear moduli are functions of temperature and moisture content. In the present study, the effects of temperature were not considered and the dependence of the elastic and shear moduli on moisture content were taken to be

¹ In (1) and elsewhere the superposed dot denotes differentiation with respect to time

$$\begin{aligned}
E_t &= E_{t0} + E_{tw}(w_f - w) \\
E_r &= E_{r0} + E_{rw}(w_f - w) \\
E_l &= E_{l0} + E_{lw}(w_f - w) \\
G_{tr} &= G_{tr0} + G_{trw}(w_f - w)
\end{aligned}$$

where the parameters E_{t0} , E_{tw} , E_{r0} , E_{rw} , E_{l0} , E_{lw} , G_{tr0} and G_{trw} are experimentally determined base values; w_f , the fiber saturation moisture content (taken to be 0.3 here); and w , the current moisture content.

The moisture induced strain component in (1) was taken to be

$$\dot{\boldsymbol{\varepsilon}}_w = \boldsymbol{\alpha}\dot{w}$$

where $\boldsymbol{\alpha}$ is the vector of moisture-induced strain coefficients

$$\boldsymbol{\alpha} = \left\{ \alpha_t \quad \alpha_r \quad \alpha_l \quad 0 \quad 0 \quad 0 \right\}^T$$

and \dot{w} is the rate of moisture content change below the fiber saturation point.

The final form of the constitutive relationship used in the model is found by multiplying (2) by the inverse of the compliance matrix (here denoted \mathbf{D}) to yield

$$\dot{\boldsymbol{\sigma}} = \mathbf{D}(\dot{\boldsymbol{\varepsilon}}_e - \dot{\mathbf{C}}\boldsymbol{\sigma})$$

From (1)

$$\dot{\boldsymbol{\sigma}} = \mathbf{D}\dot{\boldsymbol{\varepsilon}} - \boldsymbol{\sigma}_0 \tag{6}$$

where $\boldsymbol{\sigma}_0 = \mathbf{D}(\dot{\boldsymbol{\varepsilon}}_w + \dot{\mathbf{C}}\boldsymbol{\sigma})$ is a pseudo-stress vector that reflects changes in moisture content.

It should be noted that the constitutive relation (6) holds at each point within a piece of wood and hence corresponds to the local $t-r-l$ coordinate system associated with that point. In a finite element formulation, these local forms of the constitutive relations must be transformed into forms associated with the global $x-y-z$ coordinate system. Generally (as was done in the present study), an assumption is made with respect to geometry of growth rings, and from this assumption a series of orthogonal transformations can be derived and applied to (6). The details

of this procedure are omitted here for brevity; readers interested in a full description of the required orthogonal transformations are referred to Ormarsson *et al.* (1998).

2.2. Diffusion Model

Changes in moisture content within a deck board are the result of water diffusion into and out of the interior of the piece, a process assumed here to be governed by Fick's law of diffusion:

$$\frac{\partial w}{\partial t} = \nabla \cdot (D_w \nabla w) \quad (7)$$

where D_w is a diffusion coefficient that can vary spatially. It will be observed that the diffusion model (7) does not take into account the directional dependence of moisture transport in wood or variation in the rates of moisture transport across early and late wood (Claesson and Arfvidsson 1992, Perre *et al.* 1993, Ranta-Maunus 1994). Incorporating these complex effects into a more comprehensive diffusion model is the subject of continuing work.

2.3. Finite Element Systems

The mathematical formulation of a finite element system typically involves a weighted residual approach that minimizes the error made in approximating the governing differential equation for the problem considered. A full discussion of this procedure is beyond the scope of this paper and hence only the final forms of the finite element systems that apply to the structural model and diffusion model will be presented. For the structural model

$$\mathbf{K}_\sigma \mathbf{u} = \mathbf{P}_0 \quad (8)$$

where \mathbf{K}_σ is a structural stiffness matrix; \mathbf{u} , a vector of nodal displacements; and \mathbf{P}_0 , a pseudo-load vector that accounts for changes in moisture content. It should be noted that in (8) it has been assumed that body forces and surface tractions are absent. In (8) the unknown quantity is the vector of nodal displacements \mathbf{u} . In the solution phase of the analysis, the components of this vector are found and in turn, the strains, and hence the stresses, can be calculated.

For the diffusion model

$$\mathbf{C}_w \dot{\mathbf{w}} + \mathbf{K}_w \mathbf{w} = 0 \quad (9)$$

where C_w is a diffusion capacity ; and K_w is a conductivity matrix (involving diffusion coefficients); \dot{w} , a vector of rate of change of nodal moisture contents; and w , a vector of nodal moisture contents.

The system for the diffusion model (9) is an example of a transient system. The solution of such systems requires an integration scheme in which the unknown (in this case, w) is found at discrete times within the time domain. As noted, non-linear effects due to plasticity, creep and the mechano-sorptive effect were neglected in the structural model. This implies that once (9) has been solved, the structural model (8) can be solved explicitly.

2.4. Model Geometry, Mesh and Boundary Conditions

The finite model that was developed represents a two-dimensional cross-section of a typical 50.8 mm by 152.4 mm (2 in by 6 in) deck board. The geometry of the model is shown in Fig. 1. The pith corresponded to Point O and hence was taken to lie below the board. The parameters a and b were set to 0 and 177.8 mm respectively based on the typical size of trees used to mill deck pieces. As ray cells have been shown to play a key role in water transport and check initiation in softwoods (Mackay 1973, Siau 1984) an attempt was made to model the influence of these cells and hence, five rays were incorporated into the model. From Fig. 1 it can be seen that these rays follow radial lines from Point O to the top surface of the board. The number and location of these ray cells was chosen arbitrarily on the basis of some experimental observations of check locations in southern pine boards.

The cross-section was assumed to lie a significant distance from the ends of the board. In general, when such an assumption is made in two-dimensional elasticity problems, the material on either side of the cross-section is considered to constrain out-of-plane normal strains and a condition known as plane strain is said to exist.

The finite element program ANSYS[®] (2010) was used to create the checking model presented in this paper. The coupled diffusion/structural problem was solved using the multiple physics option of this program. While the coupling in the model described here can be considered one-way, in the sense that the structural model does not influence the diffusion model, the multiple physics option of ANSYS provides an efficient means of solving problems where the coupling is multi-directional.

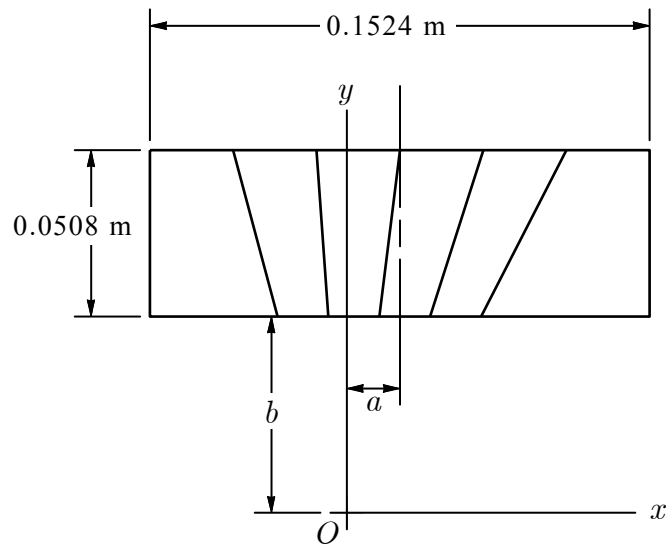


Figure 1. Model geometry

The finite element mesh is shown in Fig. 2. This mesh consists of 12,931 nodes and 12,547 elements. A four node isoparametric element with linear shape functions was used for both the diffusion model and the structural model. Since a dedicated diffusion element is not available in ANSYS, the diffusion model was solved using a thermal element by taking advantage of the similarity between Fick's law of diffusion and Fourier's law of heat transfer and adjusting the physical constants accordingly. In Fig. 2 it can be seen that the mesh was more highly refined at the top surface and along the ray cells. This was to more accurately model the higher moisture content gradients in these regions. Several mesh configurations of varying element size and refinement were investigated to ensure a converged result. In the final model shown, the element sizes in the highly refined regions were approximately 0.00025 m and the element sizes in the interior of the model were approximately 0.00075 m.

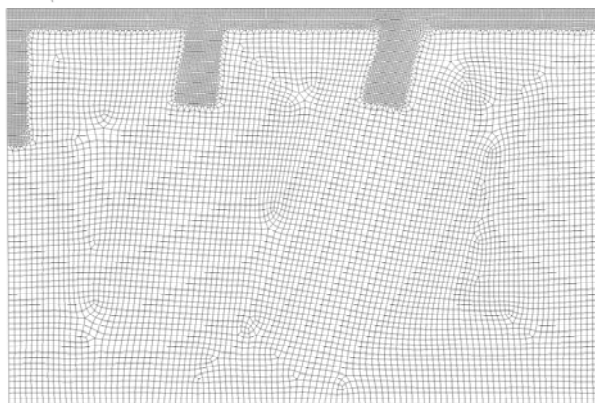


Figure 2. Finite element mesh

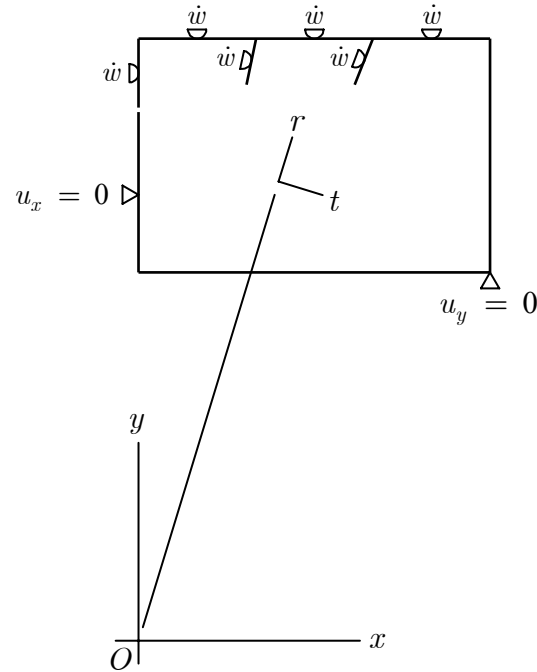


Figure 3. The finite element model boundary conditions. The triangular symbols represent structural constraints; the semi-circular symbols represent the imposed moisture contents from the assumed wet/dry cycle

Because the pith was assumed to lie below the center-line of the model, it was possible to exploit symmetry and model one-half of a deck piece. To illustrate the structural and diffusion boundary conditions the boundary of the model is shown in Fig. 3. In the diffusion model, a moisture content corresponding to a given point in the wet/dry cycle was applied to the top surface and along the ray cells. The left side of the model below the ray cell was made non-porous to ensure symmetry across the y -axis. Similarly, the right side and bottom of the model were made non-porous to prevent an exchange of moisture to or from the environment along these surfaces. In the structural model, displacement constraints in the x -direction were applied along the left end to simulate symmetry across the y -axis and a single displacement constraint in the y -direction was applied to prevent rigid body motions.

As noted, the finite element formulation for a diffusion model (9) represents a transient system. An implicit Euler backward integration scheme was used to solve this system. While this scheme can be considered unconditionally stable, solution accuracy demands that the time step be limited to

$$\Delta t_{\min} > \frac{\delta^2}{4D_w}$$

where δ is the minimum element size in the direction of maximum moisture content change and D_w , the diffusion coefficient (taken to be $7 \times 10^{-10} \text{ m}^2/\text{s}$ in this study). Hence for the minimum element size (0.00025 m) noted previously, the minimum time step was of the order of 22 seconds. This time step was sufficiently small for the rapidly changing cycles of the surface moisture content history to be investigated.

The elastic and shear moduli, Poisson's ratios and diffusion moisture induced strain coefficients used in the model were taken from (Ormarsson *et al.* 1999) and correspond to Norway spruce (*Picea abies*). These properties are listed in Table 1.

Table 1. The material properties used in the finite element model. Elastic and shear moduli are in units of MPa; r is in meters.

Property	Orthotropic direction/plane			
	Transverse	Radial	Longitudinal	Transverse/Radial
E_0	220	400	$9700 + 10^5 r$	
E_w	1300	2200	21000	
G_0				25
G_w				72
ν				0.55
α	0.35	0.19	$0.0071 - 0.038r$	

3. Results and Discussion

In a previous publication we described the development of a new type of weatherometer (accelerated check tester, ACT) and associated weathering cycles that accelerate the surface checking of realistic-sized decking boards (Rat u and Evans 2008). The initial weathering cycle that we developed exposed restrained decking boards to 12 wet and dry cycles each day. Each wet and dry cycle involved spraying samples with 12 mL of filtered water and then drying the samples using infra-red radiation and desiccated air for 30 minutes. At the end of the twelve 30 minute 'wet and dry cycles', boards were removed from the weatherometer, exposed to UV radiation and floated on water for 1.5 hours to recreate a moisture gradient between the upper and lower surfaces of the boards. Each board was then stored in a conditioning room or freezer overnight. This daily cycle was repeated for 5 days. Subsequently, we modified this weathering cycle as follows: 1, The amount of water sprayed on to the surface of the decking board sample every 30 minutes was increased from 12 to 18 mL ; 2, After the twelve 30 minute wet and dry cycles, boards were subjected to a prolonged wet-cycle during which specimens were sprayed

with 18 mL of water every 10 minutes for 1.5 h (at ambient temperature). This modified cycle increased the severity of checking in decking board samples compared to the original cycle (Ratu 2009) and we decided to use our finite element model to try to understand why the modifications to the cycle increased checking. The surface moisture contents of decking board samples were measured with an electrical moisture meter at two different points towards the end of the 6 hour series of wet and dry cycles (Fig. 4a, b), immediately at the end of the wet cycle (Fig. 4c) and after samples had dried overnight (Fig. 4d). Figure 4 shows the surface moisture contents of the wood at different times during the daily weathering cycle. Immediately after samples were sprayed with 18 mL of water during the short wet and dry cycles the surface moisture content of each board rose to ~21% (Fig. 4a). The surface moisture content dropped to ~7% after 30 minutes drying (Fig. 4b). At the end of the long (1.5h) wet cycle during which boards were sprayed with water every 10 minutes the moisture content of the measured board rose to 26% (Fig. 4c). The moisture content of the board dropped to 10% after it was allowed to dry overnight (Fig. 4d).

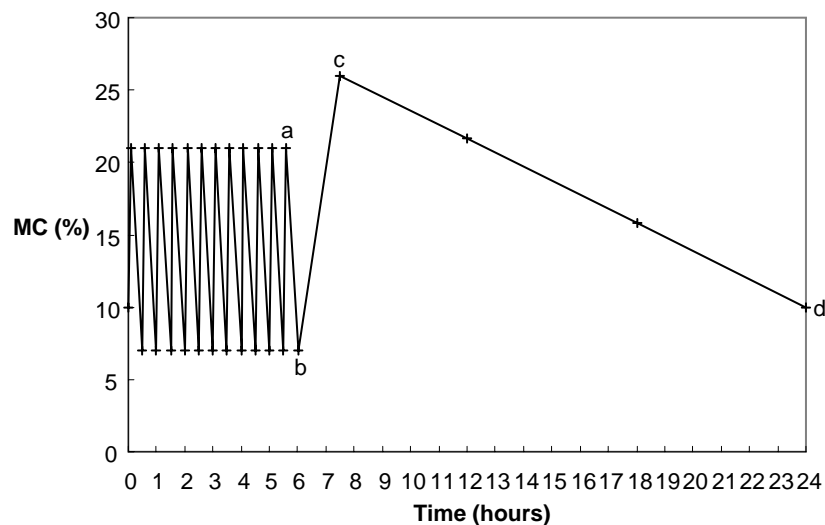


Figure 4. Measured surface moisture contents versus time for boards during accelerated weathering

To investigate the response of the finite element model to the rapidly changing conditions shown in Fig. 4, the measured surface moisture content history was input as the moisture content boundary condition. The initial moisture content of the board was set to 10%. The internal moisture content contours corresponding to points a, b, c and d in Fig. 4 are shown in Figs. 5 to 8. Since it has been suggested that transverse elastic strain (see Fig. 3) predicts the development of checks (Oliver 1986), this component of strain was plotted in Figs. 9 to 12 for points a to d of the surface moisture content history for discussion purposes. It must be emphasized that the absolute values of the strains shown in these figures may not be completely accurate given

limitations of the current model (discussed in the next section) and the assumed material properties. However, the relative values of the strains shown do provide some insight into the mechanism responsible for the formation of checks in deck boards.

Figs. 5 and 6 show the moisture content distributions in a board during the last wet (21%) and last dry (7%) cycles, respectively, of the series of twelve wet and dry cycles. The moisture contents of the interior of the board were approximately 10% for both the wet and dry cycle. However, there was considerable drying at the surface of the board and along the rays during the dry cycle. Fig. 7 shows the moisture content of the board at the end of the long (1.5 h) wet cycle (26%). Again it can be seen that the interior moisture content was approximately 10% even when the surface moisture content was 26%. However, the depth to which the moisture content exceeded the interior moisture content of 10% was greater than that in the board at the end of the short wet cycle. Fig. 8 shows the moisture content distribution at the end of the long drying cycle when the board had a surface moisture content of 10%. From this figure it can be seen that the moisture contents near the top surface and along the rays, and in the bottom half of the board were 10%. However, a region of the board extending from just below the top surface to approximately the mid-plane remained above 10% moisture content.

Figs. 9 and 10 show the transverse elastic strain distributions in a board during the last wet and last dry cycles, respectively, of the series of twelve wet and dry cycles (points a and b in Fig. 4). Fig. 9 shows that the strain was mainly compressive throughout the board when the surface moisture content was 21%. The greatest compressive transverse strain and gradient for this strain occurred near the upper board surface. Despite the overall compressive strain, Fig. 9 shows that highly localized tensile strain developed along and at the ends of the rays. Given the experimental observations of Oliver (1986) such tensile strain would be expected to cause checking along the rays. Fig. 10 shows that the transverse strain was again mainly compressive when the surface moisture content was 7%. However, in contrast to Fig. 9, it can be seen that tensile strain developed near the top and bottom surfaces of the deck board. It can also be seen that the largest compressive strain occurred along and at the ends of the rays. Fig. 11 shows that the transverse strain was again mainly compressive when the surface moisture content was 26% at the end of the long (1.5 h) wet cycle. As in Fig. 9, the tensile strain occurred at the ends of the rays. However, these regions of tensile strain at the end of the long wet cycle are considerably larger than that in the rays at the end of the short wet cycle (Fig. 9). In fact, for the centre ray and ray next to it, the regions of tensile strain appear to have joined, creating a contiguous region of tensile strain. Such tensile strain would tend to promote internal cracking and may explain why the addition of a long wet cycle increased checking of boards in our accelerated check tester (Ratu 2009). In contrast to the short wet cycle the regions of tensile strain along the centre ray and the ray next to it start at a greater distance below the surface. Also there is no tensile strain along the rightmost ray. Fig. 12 shows the transverse elastic strain at the end of the daily cycle when the surface moisture content of the board was 10% (the initial moisture content for the

whole of the board). As in previous cases, there are large regions of compressive strain. As was observed previously (Fig. 9) the tensile strain was greatest at the upper surface. However, in contrast to that and the other cases, a relatively large region of tensile strain (although of lower magnitude) developed near the centre of the board. It can also be seen that the region of highest compressive strain occurred about mid-way between the region of tensile strain and the upper surface.

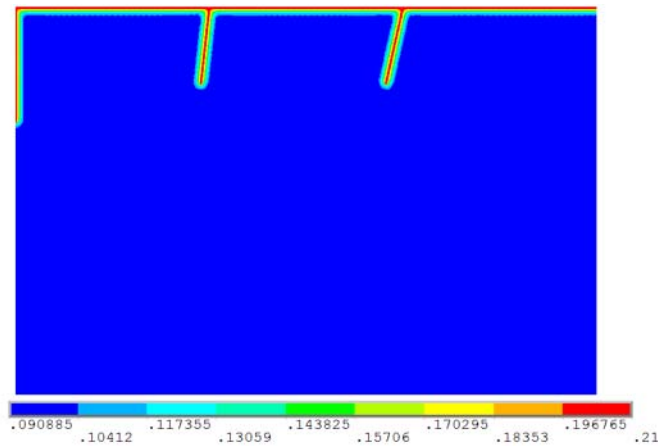


Figure 5. Moisture content contours for $t = 5.58$ hrs, at the end of a short wet cycle (point a in Fig. 4). Note the high moisture content at the surface of the board and along the rays

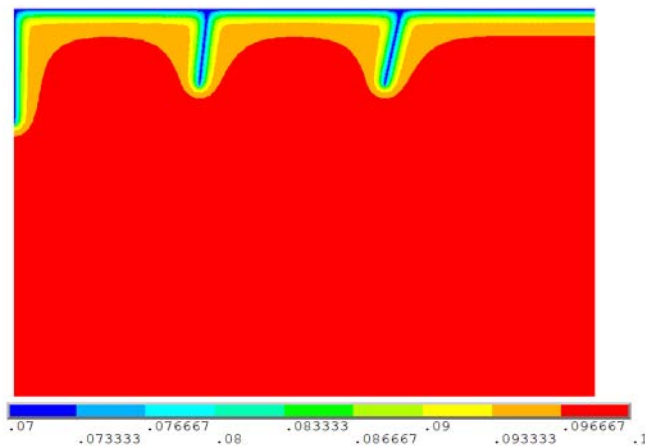


Figure 6. Moisture content contours for $t = 6.0$ hrs, at the end of a short (30 min) dry cycle (point b in Fig. 4). Note the drying of the surface layers of the board

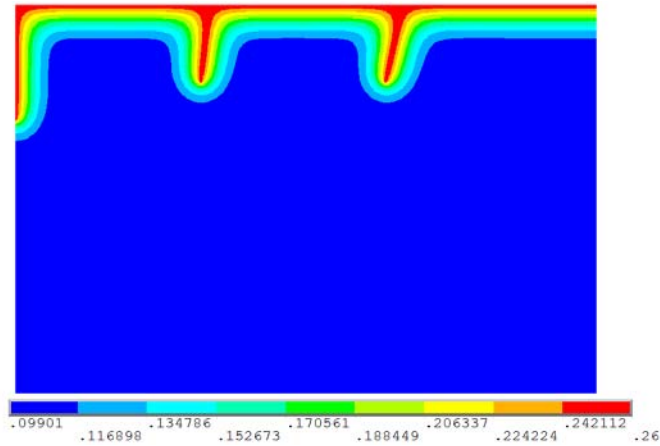


Figure 7. Moisture content contours for $t = 7.5$ hrs, at the end of a long (1.5 h) wet cycle (point c in Fig. 4). Note the very high moisture contents at the surface of the board and along the rays

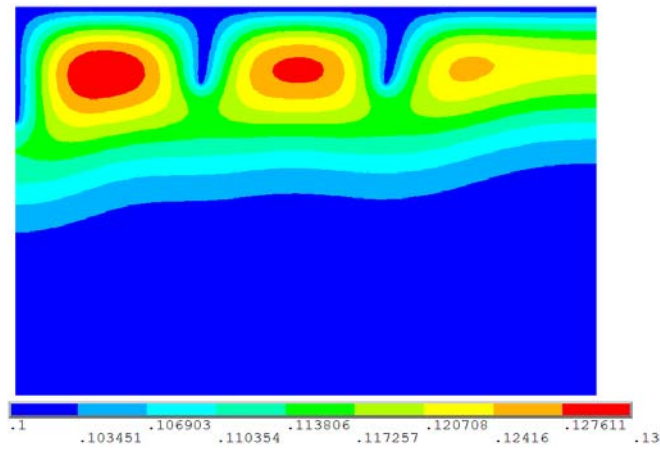


Figure 8. Moisture content contours for $t = 24$ hrs, at the end of the overnight drying (point d in Fig. 4). Note the higher sub-surface moisture contents

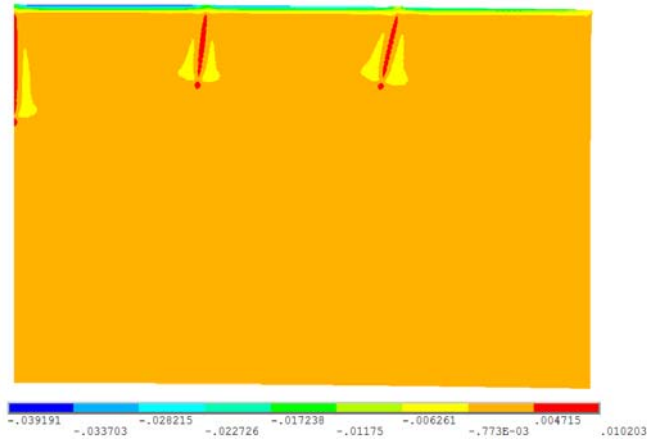


Figure 9. Transverse elastic strain contours for $t = 5.58$ hrs, at the end of a short wet cycle (point a in Fig. 4). Note the localized tensile strains along and at the ends of the rays

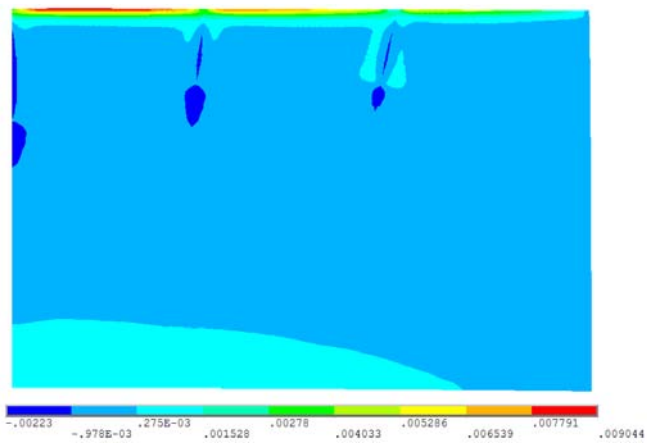


Figure 10. Transverse elastic strain contours for $t = 6.0$ hrs, at the end of a short dry cycle (point b in Fig. 4). Note the high tensile strains at the surface of the board

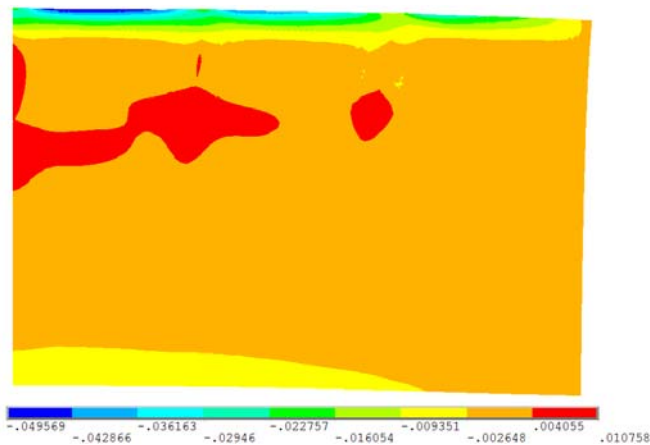


Figure 11. Transverse elastic strain contours for $t = 7.5$ hrs, at the end of a long (1.5 h) wet cycle (point c in Fig. 4). Note the high sub-surface tensile strains

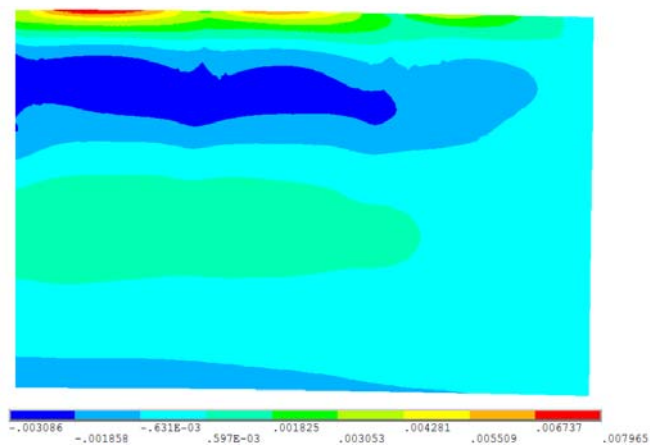


Figure 12. Transverse elastic strain contours for $t = 24$ hrs, at the end of an overnight drying (point d in Fig. 4). Note the high surface tensile strains, the lower tensile strain in the center of the board and the region of high sub-surface compressive strain

4. Conclusions

The finite element model described here predicts the development of high surface tensile strains that develop when decking boards dry. These strains clearly play an important part in the initiation of surface checks, as others have suggested (Schniewind 1963). Strains also develop when wood absorbs moisture. These strains are compressive at the surface of decking boards, but our model has shown that high tensile strains develop in the rays and in the core of boards. These high tensile strains in rays probably explain why checks propagate radially along the rays in flat-

sawn boards. The high tensile strains that develop in the core of boards may explain the development of internal checks in decking boards, and how large cracks can develop in decking boards as a result of surface and internal checks coalescing (Zahora 2000). Previous explanations of the checking of decking boards exposed outdoors have largely overlooked the importance of the tensile stresses that develop in rays and in the core of boards when they become wet. It appears likely that such strains play a very important role in the development of checks, which would explain why water repellents are so effective at preventing the checking of wood exposed outdoors (Zahora 2000 and Evans *et al.* 2003, 2009).

The finite element model described here is in the early stages of development. Nevertheless, the model has provided useful insights into the mechanism of the checking of wood and it can already be used as a virtual tool to optimize the weathering cycles in the accelerated check tester that we have developed (Ratun and Evans 2008). The model could also be used to predict the ability of water repellent treatments to reduce the development of stresses that cause checking, using known information on moisture gradients of treated wood exposed outdoors.

Our finite element model, however, has a number of limitations, which we will seek to overcome in future. Future work to improve the model will include the following: (1) Incorporation of a more realistic material model that accounts for the mechano-sorptive effect that has been shown to play an important role in the development of checks in wood during kiln drying (Salin 1992); (2) Development of a more realistic failure criterion. Failure criteria for wood under multi-axial states of stress have been, and continue to be developed (Tsai and Wu 1971). However, these criteria apply to macroscopic behavior and it is not clear if they apply to the initiation of checks which, as noted above, have been observed to initially develop in the rays; (3) Incorporation of a more realistic diffusion model. Diffusion of water in wood is a complex process that depends on spatial and temporal factors. Further, capillary action within rays influences the transport of water into and out of deck boards; (4) Experimental verification of the finite element model. Experimental verification of the numerical model is required to ensure that the predicted results, and results from any virtual prototyping scheme that might be used to mitigate deck checking, are reliable. Magnetic resonance imaging may prove to be a useful tool to examine the distribution of moisture in decking boards exposed to artificial accelerated or natural weathering.

5. References

- ANSYS®. 2010. Academic Research, Release 11.0, Documentation for ANSYS, Elements Reference.
- Claesson, J., Arfvidsson, J. 1992. A new method using Kirchhoff potentials to calculate moisture flow in wood. Proceedings of the IUFRO International Conference on Wood Drying, Understanding the wood drying process: A synthesis of theory and practice. 3:135 - 138.
- Evans, P. D., Donnelly, C. F., Cunningham, R. B. 2003. Checking of CCA-treated radiata pine decking timber exposed to natural weathering. Forest Products Journal. 53(4):66 - 71.
- Evans, P. D., Wingate-Hill, R., Cunningham, R. B. 2009. Wax and oil emulsion additives: How effective are they at improving the performance of preservative-treated wood? Forest Products Journal. 59(1/2):66 - 70.
- Mackay, J. F. G. 1973. Surface checking and drying behavior of pinus radiata sapwood boards treated with CCA preservative. Forest Products Journal. 23(9):92 - 97.
- Markarian, J. 2005. Wood-plastic composites: current trends in materials and processing. Plastics, Additives and Compounding. 7(5):20 - 26.
- McQueen, J., Stevens, J. 1998. Disposal of CCA-treated wood. Forest Products Journal. 48(11/12):92 - 97.
- Oliver, A. R. 1986. A model to correlate measurements directed towards reducing drying degrade in sawn eucalypt timber. Proceedings of the Forest Products Research Conference. 22:1 - 14.
- Ormarsson, S., Dahlblom, O., Petersson, H. 1998. A numerical study of the shape stability of sawn timber subjected to moisture variation - Part 1: Theory. Wood Science & Technology. 32(5):325 - 334.
- Ormarsson, S., Dahlblom, O., Petersson, H. 1999. A numerical study of the shape stability of sawn timber subjected to moisture variation - Part 2: Simulation of drying board. Wood Science & Technology. 33(5):407 - 423.
- Perre, P., Moser, M., Martin, M. 1993. Advances in transport phenomena during convective drying with superheated steam and moist air. Int. J. of Heat and Mass Transfer. 36(11):2725 - 2746.
- Ranta-Maunus, A. 1994. Computation of moisture transport and drying stresses by a 2-D FE programme. Proceedings of the IUFRO international wood drying conference: Improving wood drying technology. 4:187 - 194.
- Ratu, R. 2009. Development and testing of a weatherometer to accelerate the surface checking of wood. M.Sc. Thesis, University of British Columbia, 144 pp.

- Ratu, R., Evans, P. D. 2008. Development of a weatherometer to accelerate the surface checking of wood. Int. Res. Group on Wood Protection Doc IRG/WP 08-20388.
- Salin, J-G. 1992. Numerical prediction of checking during timber drying and a new mechano-sorptive creep model. *Holz als Roh- und Werkstoff*. 50(5):195 - 200.
- Schniewind, A. P. 1963. Mechanism of check formation. *Forest Products Journal*. 13(11):475 - 480.
- Siau, J. F. 1984. *Transport Processes in Wood*. Springer Series in Wood Science. Springer-Verlag, Berlin. 245 pp.
- Tsai, S. M., Wu, E. M. 1971. A general theory of strength of anisotropic materials. *Journal of Composite Materials*. 5:58 - 80.
- Zahora, A. R. 2000. Long-term performance of a "wax" type additive for use with water-borne pressure preservative treatments. Int. Res. Group on Wood Preservation Doc. IRG/WP/00-40159.